Heliyon 10 (2024) e39161

Contents lists available at ScienceDirect

Heliyon

journal homepage: www.cell.com/heliyon

Research article

Co-application of silicon and biochar affected anatomical and biochemical properties of corn leaf (*Zea mays* L.) under soil nickel toxicity

Ehsan Bijanzadeh [a,*], Hamid Reza Boostani [b], Ailsa G. Hardie [c], Mahdi Najafi-Ghiri [b]

[a] *Department of Agroecology, College of Agriculture and Natural Resources of Darab, Shiraz University, Darab, Iran*
[b] *Department of Soil Science, College of Agriculture and Natural Resources of Darab, Shiraz University, Darab, Iran*
[c] *Department of Soil Science, Faculty of AgriSciences, Stellenbosch University, Private Bag X1, Matieland, 7602, South Africa*

ARTICLE INFO

Keywords:
Heavy metal
Chlorophyll content
Metaxylem area
Membrane stability index
Relative water content
Stomata area

ABSTRACT

Soil pollution with heavy metals is a threat to crop production. Practically, application of silicon (Si) with biochar can be a cost-effective approach to immobilize metals in contaminated soils. Investigation of the anatomical and biochemical changes of corn leaf is important for describing the mechanisms of Si and biochar soil application in alleviating the negative effects of nickel (Ni) toxicity. A factorial pot experiment was conducted to investigate the effect of Si (0, 250 and 500 mg Si kg^{-1} soil) in combination with rice husk biochar (RHB) or sheep manure biochar (SMB) prepared at two pyrolysis temperatures (300 and 500 °C) on anatomical and biochemical properties of corn leaves in a Ni-polluted soil. The length, width, area and weight of third-leaf, and metaxylem and protoxylem of midrib improved by application of Si250 with RHB more than SMB. At Si250, RHB300 and RHB500 improved the stomatal area by 31.7 and 27.7 % compared to control (without biochar), respectively. The leaf membrane stability index was increased by increasing Si application level and reached 69 % in RHB300. In contrast to total chlorophyll, the highest carotenoid content, catalase and peroxidase was obtained by control (without Si and biochar) followed by SMB. At Si250, the highest relative water content (RWC) was observed in RHB300 by 34.8 % increase. Also, RHB300 had the highest total dry matter, with increases of 82.2, 120.0 and 83.1 % at Si0, Si250 and Si500, respectively. By increasing the Si level and biochar application, the shoot Ni decreased between 42.1 and 133.3 %. Combined application of Si250 with RHB300 resulted in the highest dry matter through improving the leaf dimensions, metaxylem and protoxylem areas of midrib, membrane stability index, total chlorophyll, and RWC, while Ni uptake was reduced.

1. Introduction

Corn (*Zea mays* L.) is one of the main important staple crops in the world, and together with wheat and rice, provide at least 30 % of the food calories to more than 4.5 billion people in 94 developing countries [1]. In Iran, corn is one of the main and strategic crops which is cultivated as a fodder crop for livestock production. In the 2020–2021 growing season, more than 241 thousand hectares were cultivated for corn in Iran, which produced over 2 million tons of corn [2].

* Corresponding author.
E-mail address: bijanzd@shirazu.ac.ir (E. Bijanzadeh).

https://doi.org/10.1016/j.heliyon.2024.e39161
Received 27 July 2024; Received in revised form 8 October 2024; Accepted 8 October 2024
Available online 9 October 2024

Due to ongoing urbanization and industrialization, soil pollution by heavy metals is rapidly increasing which results in many detrimental effects on ecosystems [3]. Heavy metal toxicity in agricultural soils is a major concern due to their persistent toxicity effects in soils and organisms [4,5]. The potentially toxic heavy metal, Nickel (Ni), is also considered a critical plant micronutrient which is needed for photosynthesis and vegetative and reproductive growth of corn [6].

Soil Ni toxicity creates negative effects on crop morphophysiological properties and directly decreases seed germination, chlorophyll contents, plant height, nutrient uptake, and biomass production, subsequently reducing crop yields or resulting in plant death [6,7]. Excessive Ni in plant tissues results in the generation of reactive oxygen species (ROS) like peroxides and superoxide, resulting in oxidative damage of plant organelles which induces enzyme activity [8]. Furthermore, Ni toxicity disrupts plant physiology by decreasing the size of the vascular bundles and stomata, the thickness of the mesophyll, and the plasticity of cell walls, resulting in electrolyte leakage and decreasing leaf membrane stability index [8,9].

Like other plant stresses, such as water or salt stress, heavy metals toxicity can negatively affect leaf anatomy and mesophyll cells [10–12]. Bijanzadeh and Kazemeini [13] reported that under stress, decreasing third-leaf surface area was due to narrower leaves and growth limitation especially between the first 5 mm above the leaf base. Maturation of mesophyll cells occurs at the first few millimeters of the leaf base (division zone), and water stress can critically slow leaf spatial distribution at this zone which limits leaf expansion. Another symptom of heavy metal toxicity in plants is a decrease in the size of stomata [14]. The reaction of stomatal size to abiotic stresses is depended on crop type, leaf relative water content (RWC), light intensity, nutrient uptake and the other environmental conditions [15,16].

A practical strategy to reduce the detrimental impacts of heavy metal toxicity in plants is the application of silicon (Si). Cereals are among the highest Si accumulators within the monocots; where Si can bond with heavy metals to sequester them in apoplastic pathways in the crop structure [17]. Although not entirely understood, exogenous Si application benefits crops grown under heavy metal stress by increasing cell wall strength and photosynthetic pigment content, creating more erect and elongated leaves, thus enhancing light interception [18]. Tripathi et al. [19] found that Si upregulates genes that alleviate the detrimental impacts of heavy metals in rice by changing the root and shoot structure. As biochar and Si have different positive effects on the mitigation of soil heavy metals on crops, they could be applied together to enhance crop production in polluted soils. In rice, application of silicon-rich biochar reduced shoot Cd uptake more than application of biochar alone [3].

Remediation of Ni contaminated soils using organic amendments such as biochar has been recommended as compared to the use of inorganic amendments due to their higher safety, low cost and improvement in soil characteristics [11,20,21]. The pyrolysis temperature of crop residues (200–900 °C) for the production of biochar is a critical parameter influencing the porous features of the biochar. Depending on type of crop residue, pyrolysis temperature and soil conditions, biochar can be a suitable adsorbent for detoxifying of many heavy metals in agricultural ecosystems [7,20]. Biochar with high surface area can immobilize heavy metals through trapping them in its nanopores [9]. The polar functional groups in biochar can immobilize heavy metals through electrostatic interactions and complexation mechanisms, while the alkalinity and ash in biochar can promote precipitation. Biochar application in contaminated soils can increase corn growth, dry matter production and decreased accumulation of toxic metals [22,23].

As the Ni concentration is increasing in the agricultural soils of Iran due to the extensive use of sewage sludge and wastewaters [24], it is necessary to inhibit Ni uptake and toxicity to ensure safe food production [5]. Based on the scientific literature, we hypothesized that Si and biochar soil application by changing the anatomical and biochemical changes of corn leaf can mitigate the detrimental effects of potentially toxic elements (PTEs) such as Ni. At the present time, little is known about the primary effects of Si with biochar on anatomical and biochemical changes of corn leaf under Ni toxicity. Therefore, the main aim of the current study was to investigate the combined effect of Si and biochar application produced from different crop residues (rice husk and sheep manure) and pyrolysis temperatures (300 and 500 °C) on anatomical and biochemical properties of the corn leaf cultivated in a Ni-polluted soil.

2. Materials and methods

2.1. Soil preparation and treatments

A calcareous, sandy loam topsoil (0–20 cm) classified as Calcaric Cambisols (Loamic, Ochric) according to WRB [25], was collected from an agricultural field in southern Iran (28°45′0.99″N 54°26′52.14″E, Elevation 1105 m). After air-drying of the soil and passing through a 2 mm sieve, the sample was analyzed to determine its general physical and chemical properties which are given in Table 1. The soil was a calcareous soil with alkaline pH and low organic content. Initially, soil samples were contaminated with Ni levels

Table 1
Selected physicochemical characteristics of the soil before cultivation.

Sand (%)	58.00	Available K (mg kg^{-1})	251.00
Silt (%)	30.00	Available P (mg kg^{-1})	13.00
Clay (%)	12.00	CEC ($cmol_{(+)}kg^{-1}$)	11.70
Soil textural class	Sandy loam	Fe-DTPA (mg kg^{-1})	4.64
$pH_{(s)}$	7.59	Mn-DTPA (mg kg^{-1})	12.30
EC (dS m^{-1})	2.60	Cu-DTPA (mg kg^{-1})	1.33
CCE (%)	55.00	Zn-DTPA (mg kg^{-1})	0.64
OM (%)	0.50	Ni-DTPA (mg kg^{-1})	0.39

Notes: EC, electrical conductivity; OM, organic matter; CCE, calcium carbonate equivalent; CEC, cation exchange capacity.

according to the experimental design. Specifically, 2 kg of soil was placed in a thick plastic bag. Subsequently, 1000 mL of an aqueous solution containing Ni prepared from nickel chloride (NiCl2) and distilled water, was added to the soil samples. The mixture was thoroughly combined to achieve Ni concentration 300 mg kg−1 of soil. The samples were then allowed to dry at room temperature. Following this, they were ground into a powder, and their moisture content was adjusted to field capacity using distilled water, which was measured by weight. The samples were then incubated at room temperature to dry. The wetting and drying cycles of the soil samples were repeated three times to reach an equilibrium state and to simulate actual field conditions [20]. Si solutions were prepared using Na2SiO3 and were added to the soil according to the experimental design (0, 250, or 500 mg/kg Si). The amount of moisture required to bring 2 kg of dry soil to its field capacity was also considered, and the mixture was blended until uniform [3,18].

2.2. Biochar production and its characteristics

Biochars were prepared from rice husks and sheep manure. Prior to pyrolysis, the organic substrates were air-dried and ground, and then placed in an oven for 24 h at 105 °C. The dried and ground biomass was then subjected to slow pyrolysis in an electric muffle furnace (Shimifan, F47) at temperatures of 300 and 500 °C under limited oxygen conditions. The temperature was gradually increased from room temperature by 5 °C per minute until it reached the final temperature, which was maintained for 2 h to facilitate slow pyrolysis. The prepared biochars were allowed to cool slowly and passed through a 0.5 mm sieve.

The chemical properties of the biochars produced were assessed through a series of standardized procedures. The pH was determined by mixing 1.0 g of the biochar sample with 20 mL of deionized water, agitating the mixture at 40 rpm for 1 h, and subsequently measuring the pH with a pH meter [26]. Electrical conductivity (EC) was evaluated using a 1:20 ratio of biochar to deionized water, with the mixture shaken for 30 min [27]. The concentrations of C, N, and H in the biochar samples were analyzed utilizing a CHN analyzer (ThermoFinnigan Flash EA 1112 Series). Cation exchange capacity was measured via the ammonium acetate method, which involved adding 20 mL of 1M NH_4OAC at pH 7.0 to 4 g of the biochar sample, shaking the mixture for 1 h, filtering it through Whatman 42 filter paper, and subsequently quantifying the concentrations of Ca, Mg, Na, and K in the filtrate [28]. The total concentrations of Ni, iron, manganese, copper, and zinc were determined through atomic absorption spectroscopy (PG 990, PG Instruments Ltd., UK) following ashing at 550 °C and acid dissolution. Total phosphorus (P) was quantified in the acid-digested ash fraction using the molybdate-ascorbic acid method, with spectrophotometric measurements taken at a wavelength of 460 nm. The ash content of the biochars was determined by heating an open-top crucible at 750 °C for 1 h. The moisture content was assessed by heating a 1.00 g sample of biochar at 105 °C in an oven for 24 h. The combined content of oxygen and sulfur was calculated by subtracting the ash, moisture, C, N, and H from the total mass. The physicochemical properties of the biochars are presented in Table 2.

2.3. Experimental design and corn pot experiment

The corn pot experiment was arranged as a factorial study using a completely randomized design (RCD) with three replicates. The first factor was Si levels [0 (Si0), 250 (Si250) and 500 (Si500) mg Si kg^{-1} soil] and the second factor was biochar treatment (with no biochar application (C), sheep manure biochar produced at 300 °C (SMB300), sheep manure biochar produced at 500 °C (SMB500), rice husk biochar prepared at 300 °C (RHB300), and rice husk biochar prepared at 500 °C (RHB500)), each applied at 3 % (w/w).

Table 2
Physical and chemical characteristics of the biochars.

	SMB300	SMB500	RHB300	RHB500
pH (1:20)	9.96 ± 0.03^{bc}	11.00 ± 0.02^{a}	9.00 ± 0.04^{c}	10.30 ± 0.03^{ab}
EC (1:20) (dS m^{-1})	3.94 ± 0.06^{b}	4.28 ± 0.04^{a}	0.84 ± 0.01^{d}	1.17 ± 0.03^{c}
CEC ($cmol_+ kg^{-1}$)	19.70 ± 0.8^{a}	18.94 ± 0.65^{a}	18.94 ± 0.35^{a}	15.33 ± 0.40^{b}
C (%)	25.40 ± 1.50^{d}	31.80 ± 2.01^{c}	45.00 ± 2.60^{b}	50.00 ± 3.50^{a}
H (%)	1.85 ± 0.09^{a}	0.80 ± 0.01^{b}	2.28 ± 0.07^{a}	1.06 ± 0.05^{b}
N (%)	2.10 ± 0.10^{a}	1.57 ± 0.15^{b}	1.30 ± 0.09^{bc}	1.10 ± 0.11^{c}
P (%)	0.36 ± 0.01^{a}	0.38 ± 0.03^{a}	0.20 ± 0.01^{b}	0.23 ± 0.01^{b}
K (%)	2.36 ± 0.01^{a}	2.47 ± 0.01^{a}	0.81 ± 0.01^{b}	1.02 ± 0.01^{b}
Fe (mg kg^{-1})	1875.00 ± 10.50^{a}	2019.00 ± 9.30^{a}	207.00 ± 3.01^{b}	358.00 ± 5.09^{b}
Mn (mg kg^{-1})	236.00 ± 2.50^{a}	241.00 ± 2.75^{a}	105.00 ± 1.60^{c}	139.00 ± 1.53^{b}
Cu (mg kg^{-1})	20.10 ± 0.70^{a}	20.80 ± 0.90^{a}	1.50 ± 0.03^{b}	2.80 ± 0.04^{b}
Zn (mg kg^{-1})	52.10 ± 1.01^{a}	60.70 ± 1.60^{a}	18.20 ± 0.90^{b}	18.50 ± 0.70^{b}
Ni (mg kg^{-1})	3.00 ± 0.20^{b}	15.40 ± 0.6^{a}	Nd	Nd
Na (%)	0.73 ± 0.01^{a}	0.77 ± 0.01^{a}	0.06 ± 0.01^{b}	0.07 ± 0.01^{b}
Ca (%)	5.80 ± 0.08^{a}	7.50 ± 0.05^{a}	0.21 ± 0.01^{b}	0.25 ± 0.01^{b}
Moisture content (%)	1.91 ± 0.01^{b}	1.82 ± 0.01^{b}	2.65 ± 0.01^{a}	2.37 ± 0.01^{a}
Ash content (%)	53.80 ± 1.01^{a}	60.00 ± 1.60^{a}	34.20 ± 0.90^{b}	44.80 ± 0.70^{b}
H:C mole ratio	0.87 ± 0.01^{a}	0.30 ± 0.01^{b}	0.60 ± 0.01^{a}	0.25 ± 0.01^{b}
O + S:C mole ratio	0.44 ± 0.01^{a}	0.09 ± 0.01^{c}	0.24 ± 0.01^{b}	0.01 ± 0.001^{c}
C:N ratio	12.10 ± 0.10^{d}	20.20 ± 0.12^{c}	34.60 ± 0.15^{b}	45.40 ± 0.16^{a}

Notes: SMB300, sheep manure biochar prepared at 300 °C; SMB500, sheep manure biochar prepared at 500 °C; RHB300, rice husk biochar prepared at 300 °C; RHB500, rice husk biochar prepared at 500 °C; CEC, cation exchange capacity; EC, electrical conductivity; Nd, non-detectable. Means in each row with the same letter do not differ significantly by LSD test at 5 % probability level. Data presented with ±SE.

In each plastic pot, 2 kg of treated soil (with Si levels and biochars) based on the experimental design was transferred (45 experimental units), and then 6 corn seeds (cv. single cross 604) provided from Agricultural Research Center of Hasan Abad, Darab, Fars province, Iran were sown at a depth of 2 cm. After emergence, the corn seedlings were thinned to four seedlings. The greenhouse temperature was 25 ± 5 °C, with 60 ± 10 % relative humidity, and light intensity was in range from 600 to 1100 μmol m $^{-2}$ s $^{-1}$. A

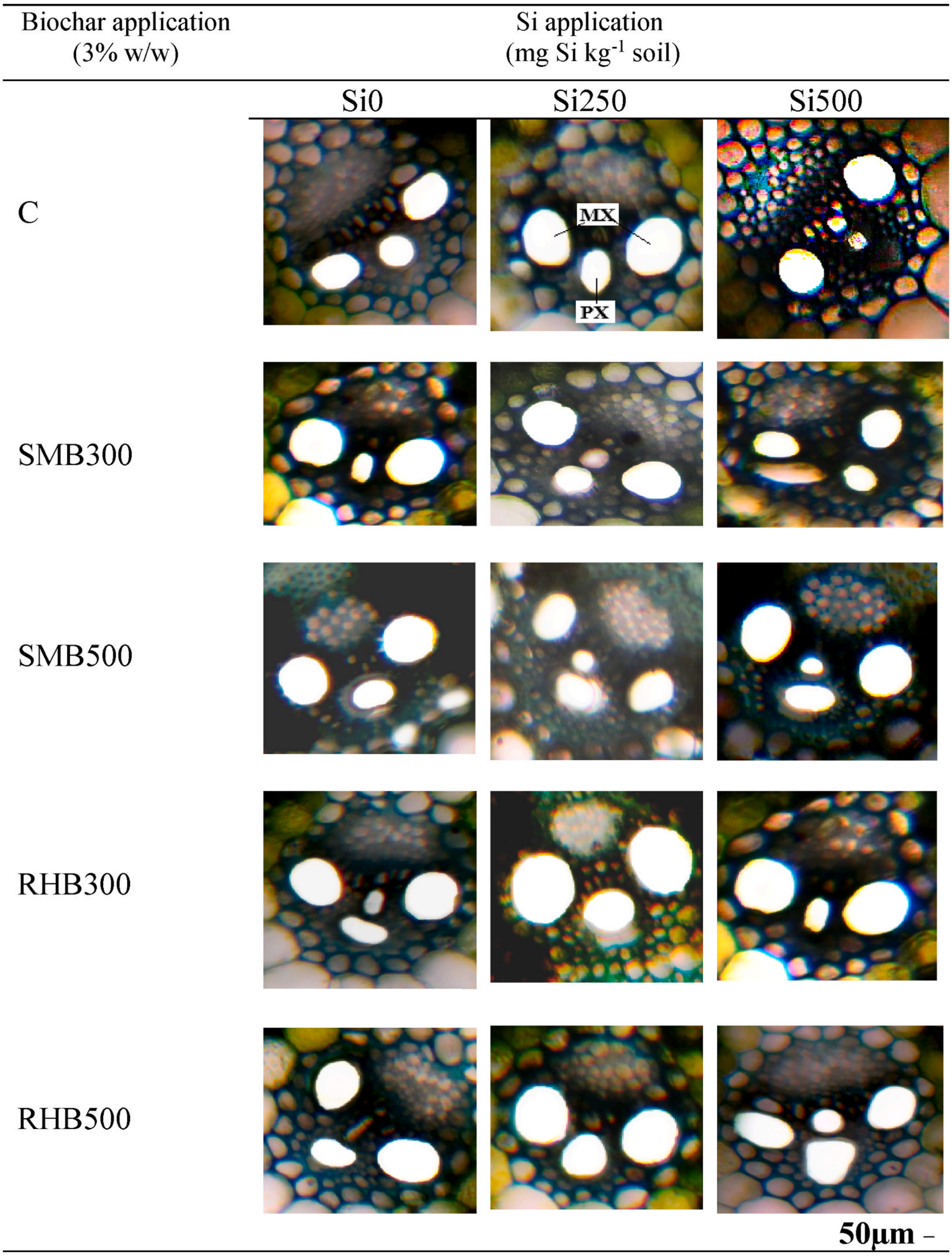

Fig. 1. The cross-sectional micrographs of the midrib of corn third-leaf including metaxylem (MX) and protoxylem (PX) grown in Si and biochar amended Ni-polluted soil. Leaf sections were taken from 5 to 7 mm above the leaf base. Scale bar represents 50 μm. MX: metaxylem, PX: protoxylem; SMB300, sheep manure biochar prepared at 300 °C; SMB500, sheep manure biochar prepared at 500 °C; RHB300, rice husk biochar prepared at 300 °C; RHB500, rice husk biochar prepared at 500 °C.

gravimetric method was used to maintain the soil moisture of pots at the field capacity level with distilled water by daily weighing. The third-leaf blades at ZGS13 stage [29] were selected to determine the anatomical and biochemical characteristics which are described below.

2.4. Third-leaf dimensions and anatomy structure

First, the leaf length and width of the third-leaf was determined by a ruler. Then, the area of third-leaf was determined by a leaf area meter (Kaiser, RS1, Germany). To study the leaf anatomy, sections were taken from 5 to 7 mm above the leaf base [30]. Segments were immediately transferred to phosphate buffered saline (PBS) supplemented with 3 % formaldehyde and incubated overnight. The leaf blades were washed in PBS and dehydrated in a graded series of ethanol [31]. Then, segments were cut with a razor and stained with 0.5 % toluidine blue (TB) for 1 min [32]. A Ceti bright field microscope was used to observe the midrib structure. Images of the midrib area (Fig. 1) and stomatal dimensions of the third-leaf (Fig. 2) were captured with a digital camera (X60 HS, Canon, Inc., Ota, Tokyo, Japan).

2.5. Stomatal measurement

The stomatal area of the third-leaf was determined with epidermal impression from the 5–10 mm above the leaf base. Fingernail varnish was applied to the adaxial (upper) leaf surface and permitted to dry. Thereafter, clear tape was applied to the hardened varnish to peel it from the leaf, and then it was placed on a microscope slide for viewing [15].

2.6. Determination of pigment contents

The chlorophyll was extracted by gradually adding 10 mL of 80 % acetone to 200 mg of third-leaf tissue while grinding with a mortar and pestle. After creating a homogenized solution as described by Arnon [33], the solution absorbance was determined by a double-beam UV–VIS spectrophotometer (UV-1900, Shimadzu, Japan) at λ = 645, 663, and 470 nm. Then, the chlorophyll *a, b* and total [33] and carotenoid [34] contents were calculated.

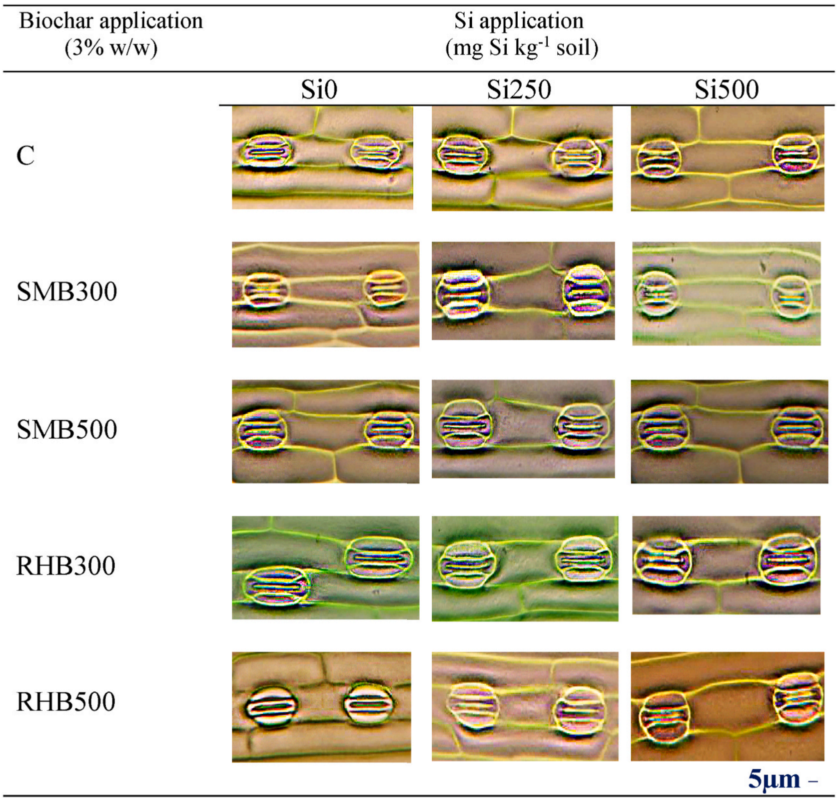

Fig. 2. Stomatal micrograph dimensions for corn third-leaf grown in Si and biochar amended Ni-polluted soil. Leaf sections were taken from 5 to 10 mm above the leaf base. MX: metaxylem, PX: protoxylem. Scale bar represents 5 μm. SMB300, sheep manure biochar prepared at 300 °C; SMB500, sheep manure biochar prepared at 500 °C; RHB300, rice husk biochar prepared at 300 °C; RHB500, rice husk biochar prepared at 500 °C.

2.7. Enzymes assay

For enzyme extraction, 0.5 g of fresh third-leaf were ground to a fine powder in liquid nitrogen by mortar and pestle and then homogenized in 2 mL extraction buffer containing 10 % (w/v) polyvinyl pyrrolidone (PVP) in 50 mM potassium-phosphate buffer (pH 8), 1 mM dithiothreitol (DTT), and 0.1 mM ethylene diamine tetra acetic acid (EDTA). Then, the catalase activity (CAT) was determined using a spectrophotometer (UV-160A) based on the method of Aebi [35], by monitoring the decrease in absorbance at 240 nm due to H_2O_2 consumption. The CAT activity was expressed as units (μmol H_2O_2 consumed per minute) per milligram of protein. The peroxidase activity (POD) was evaluated by the method of Chance and Maehly [36]. Peroxidase activity was expressed as units (μmol guaiacol oxidized per minute) per milligram of protein.

2.8. Electrolyte leakage and the leaf membrane stability index

Electrolyte leakage was evaluated using 200 mg of fresh tissue of the third leaf. Tissue was cut into 1 cm long strips and placed into screw cap test tubes with 8 mL of distilled, deionized water. Tubes were incubated in a 35 °C water bath for 30 min, and the initial electrical conductivity (EC_1) was measured using an electrical conductivity meter (Model Twin CodB-197, Metrohm, Germany). Samples were boiled at 95 °C for 20 min to release electrolytes. Samples were cooled and final electrical conductivity (EC_2) was determined [37]. The percentage of electrolyte leakage was calculated using the following equations:

$$\text{EL } (\%) = \frac{(\text{EC1})}{(\text{EC2})} \times 100 \quad [1]$$

Membrane stability index (MSI) was calculated by the following formula [38]:

$$\text{MSI } (\%) = \left[1 - \frac{(\text{EC1})}{(\text{EC2})}\right] \times 100 \quad [2]$$

2.9. Leaf relative water content (RWC) measurement

The leaf RWC was measured by the method of Machado and Paulsen [39]. Briefly, six leaf discs (10 mm in diameter) of third-leaf were taken from a fully expanded flag leaf in each pot, and were weighed for determination of fresh weight (FW). The leaf discs were placed in deionized water for 6 h and then dried on filter paper and weighed for total weight (TW). The samples were oven dried for a dry weight measurement (DW). Finally, the RWC was determined as:

$$\text{RWC} = [(\text{FW} - \text{DW}) / (\text{TW} - \text{DW})] \times 100 \quad [3]$$

2.10. Plant height and shoot dry weight

At 36 days after germination, the aboveground parts of the plants were harvested and plant height measured in the laboratory. The harvested plant material was then placed in an oven at 72 °C for 48 h and immediately weighed to determine total shoot dry weight using a digital balance.

2.11. Ni analysis

After separation of root system from the soil, the soil was air-dried and passed from a 2 mm sieve. Soil Ni availability was determined by DTPA solution (pH = 7.3). The concentration of Ni in the shoots was measured by ashing of the plant material (550 °C for 2 h) and subsequently dissolved in 2 M HCl [40]. In the obtained extract, the content of Ni was determined by an atomic absorption spectroscopy (AAS) (PG 990, PG Instruments Ltd. UK).

2.12. Statistical analysis

Data were statistically analyzed for variance using the SAS software (version 9.4) (SAS Institute, Cary, NC, USA). To check the normal distribution of data, Kolmogorov-Smirnov and Shapiro-Wilk tests were used and the skewness and kurtosis indices of data confirmed that the distribution of data was normal. When analysis of variance demonstrated a significant treatment effect (Si levels × biochar treatments), the means were compared using Fisher's Least Significant Difference (LSD) test at 5 % probability level.

3. Results

3.1. Soil characteristics

Some physicochemical characteristics of the soil before cultivation are given in Table 1. The soil texture was sandy loam and exhibited alkaline characteristics with pH = 7.59. The electrical conductivity (EC) was low (2.60 dS m^{-1}) which is suitable for corn production. Also, the soil's cation exchange capacity (CEC) was low due to the relatively low amounts of clay percent (12 %) and organic matter (0.5 %). Furthermore, the soil's available nutrient contents, including P, Fe, Zn, Mn, and Cu, were below the necessary thresholds required for the optimum growth of corn. On the other hand, the concentration of soil Ni, as extracted by DTPA (diethylenetriaminepentaacetic acid), was lower than the detection limit for corn growth.

3.2. Characteristics of the biochars

The SMB biochars were more saline (higher EC) and alkaline (higher pH) than the RHB and contained a higher proportion of ash, which increased with increasing pyrolysis temperature (Table 2). Hence the inorganic nutrients contents (P, K, Ca, Mg, Fe, Mn, Cu and Zn) were substantially higher in the SMB, also increasing with pyrolysis temperature (Table 2). In contrast, the CEC of the biochars decreased with increasing pyrolysis temperature, and SMB300 had the highest CEC value (Table 2). By increasing pyrolysis temperature, the C content of the biochars increased, but the H, O and N contents declined. This could be explained by the volatilization of N and O compounds at higher pyrolysis temperatures (Golizdah and Hu 2021). The total Ni content of the RHB was negligible, while SMB had a low content of Ni.

3.3. Leaf properties

Application of Si and biochar had a significant effect ($p \le 0.05$) on leaf dimensions and weight of the corn third-leaf in the Ni-polluted soil (Table 3). Maximum leaf length was achieved in the RHB300 and RHB500 at Si250 application rate, which differed significantly ($p \le 0.05$) from the Si0 and Si500 application rates. At Si250 level, application of RHB300 resulted in the greatest leaf width (10.8 ± 0.3 mm) with no significant difference ($p \le 0.05$) from RHB500 and SMB500 (Table 3). At the highest Si level (Si500), RHB significantly enhanced leaf width compared to SMB. At all Si levels, the temperature of biochar preparation (300 or 500 °C) had a slight effect ($p \le 0.05$) on leaf area of third-leaf, while the RHB enhanced leaf area to the greatest extent, especially at Si250. Application of RHB increased the leaf weight by 83.3, 76.4 and 65.5 % under Si0, Si250 and Si500 compared to control (no application of biochar), respectively. Overall, leaf dimensions and weight were improved to the greatest extent by application of Si250 with RHB (Table 3).

3.4. Area of midrib, metaxylem and protoxylem

The midrib area at the leaf base (division zone) is one of the main compartments of xylem structure. The cross-sectional micrographs of corn third-leaf midrib, including metaxylem and protoxylem, grown a Ni-polluted soil amended with Si and biochar are shown in Fig. 1. In all treatments, the midrib area at 5–7 mm above the leaf base usually had two metaxylems and one or two protoxylems. The number of metaxylems and protoxylems was not affected by Si and biochar application (Fig. 1), whereas the midrib area, and consequently, the area of metaxylem and protoxylem was affected ($p \le 0.05$) (Table 4). In all biochar treatments, application of Si250 increased the midrib area in comparison to the other Si levels, however RHB was superior to SMB in terms of midrib area improvement. In the absence of biochar, the midrib area in Si0, Si250 and Si500 decreased by 26.2, 21.2 and 23.8 %, compared to RHB300, respectively. By increasing the Si application level from 0 to 250 mg Si kg^{-1} soil, the metaxylem area in each biochar treatment increased significantly, but at Si500 decreased (Table 4). At Si250, RHB300 and RHB500 resulted in the highest metaxylem area. RHB300 increased the protoxylem area by 48.9, 24.4 and 20.1 % at Si0, Si250 and Si500 levels compared to control (without biochar), respectively. Overall, RHB significantly enhanced the metaxylem and protoxylem areas compared to SMB.

Table 3
Interaction effect of Si and biochar application on third-leaf dimensions and weight of corn (cv. single cross 604) in a Ni-polluted soil.

Si application (mg Si kg^{-1} soil)	Biochar application (3 % w/w)	Leaf length (mm)	Leaf width (mm)	Leaf area (mm^2)	Leaf weight (g)
Si0	C	88.3 ± 0.5^{f}	8.1 ± 0.1^{gh}	558.1 ± 3.4^{f}	0.42 ± 0.02^{g}
	SMB300	89.2 ± 0.3^{ef}	8.8 ± 0.2^{ef}	610.2 ± 3.9^{e}	0.65 ± 0.06^{e}
	SMB500	86.5 ± 0.2^{f}	9.1 ± 0.1^{de}	612.3 ± 4.1^{e}	0.66 ± 0.03^{e}
	RHB300	91.7 ± 0.3^{de}	9.6 ± 0.3^{bcd}	682.3 ± 2.3^{cd}	0.74 ± 0.03^{d}
	RHB500	96.1 ± 0.4^{bc}	9.7 ± 0.2^{bc}	720.1 ± 2.2^{c}	0.77 ± 0.02^{d}
Si250	C	93.5 ± 0.3^{cd}	9.1 ± 0.1^{de}	661.3 ± 3.5^{de}	0.51 ± 0.04^{f}
	SMB300	96.6 ± 0.2^{bc}	9.7 ± 0.1^{bc}	729.2 ± 4.5^{c}	0.78 ± 0.05^{cd}
	SMB500	99.4 ± 0.5^{ab}	10.1 ± 0.2^{abc}	781.2 ± 4.1^{b}	0.84 ± 0.03^{bc}
	RHB300	101.3 ± 0.3^{a}	10.8 ± 0.3^{a}	850.3 ± 5.3^{a}	0.90 ± 0.02^{a}
	RHB500	102.2 ± 0.4^{a}	10.4 ± 0.2^{ab}	821.7 ± 5.1^{ab}	0.88 ± 0.03^{ab}
Si500	C	91.3 ± 0.2^{de}	7.9 ± 0.1^{h}	561.6 ± 4.3^{f}	0.46 ± 0.01^{fg}
	SMB300	92.3 ± 0.2^{de}	8.3 ± 0.2^{fg}	598.1 ± 3.9^{ef}	0.64 ± 0.03^{e}
	SMB500	91.3 ± 0.1^{de}	8.6 ± 0.1^{fg}	611.4 ± 3.8^{e}	0.66 ± 0.02^{e}
	RHB300	96.8 ± 0.3^{b}	9.3 ± 0.1^{de}	701.5 ± 2.8^{cd}	0.75 ± 0.03^{d}
	RHB500	97.1 ± 0.2^{b}	9.6 ± 0.3^{bcd}	728.3 ± 3.4^{c}	0.78 ± 0.03^{cd}

Notes: SMB300, sheep manure biochar prepared at 300 °C; SMB500, sheep manure biochar prepared at 500 °C; RHB300, rice husk biochar prepared at 300 °C; RHB500, rice husk biochar prepared at 500 °C. Means in each column with the same letter do not differ significantly by LSD test at 5 % probability level. Data presented with ±SE.

Table 4
Interaction effect of Si and biochar application on area of midrib, metaxylem and protoxylem of corn third-leaf (cv. single cross 604) in a Ni-polluted soil.

Si application (mg Si kg^{-1} soil)	Biochar application (3 % w/w)	Midrib area (μm^2)	Metaxylem area (μm^2)	Protoxylem area (μm^2)
Si0	C	100461 ± 1068^{g}	11906 ± 168^{g}	6358 ± 32^{g}
	SMB300	124514 ± 1311^{de}	12365 ± 168^{ef}	8431 ± 31^{ef}
	SMB500	123017 ± 1401^{e}	12861 ± 194^{e}	8867 ± 47^{de}
	RHB300	136214 ± 1021^{b}	13552 ± 159^{d}	9361 ± 42^{cd}
	RHB500	132451 ± 1346^{bc}	13467 ± 197^{d}	9468 ± 51^{bc}
Si250	C	111545 ± 812^{f}	12033 ± 186^{f}	7986 ± 62^{f}
	SMB300	129110 ± 1365^{c}	14041 ± 192^{c}	9936 ± 29^{b}
	SMB500	128015 ± 998^{cd}	14036 ± 106^{c}	9899 ± 36^{b}
	RHB300	141663 ± 1451^{a}	15306 ± 171^{a}	11341 ± 34^{a}
	RHB500	140151 ± 1156^{a}	15441 ± 143^{a}	11045 ± 30^{a}
Si500	C	101654 ± 769^{g}	11102 ± 135^{g}	7903 ± 38^{f}
	SMB300	124102 ± 1136^{de}	13206 ± 108^{d}	9486 ± 59^{bc}
	SMB500	124255 ± 968^{de}	13286 ± 129^{d}	9467 ± 67^{bc}
	RHB300	133465 ± 1165^{bc}	14903 ± 149^{b}	10897 ± 4^{a}
	RHB500	130498 ± 1132^{bc}	14604 ± 153^{b}	10911 ± 5^{a}

Notes: SMB300, sheep manure biochar prepared at 300 °C; SMB500, sheep manure biochar prepared at 500 °C; RHB300, rice husk biochar prepared at 300 °C; RHB500, rice husk biochar prepared at 500 °C. Means in each column with the same letter do not differ significantly by LSD test at 5 % probability level. Data presented with ±SE.

3.5. Stomatal area

The stomatal micrograph dimensions of the corn third-leaf grown in a Ni-polluted soil amended with Si and biochars are presented in Fig. 2. Results showed that at Si0, the SMB300 and SMB500 could not mitigate the detrimental effect of Ni on stomatal area at 5–10 mm above the third-leaf base (Fig. 3). In contrast, at Si250, application of RHB300 and RHB500 improved the stomatal area by 31.7 and 27.7 % compared to control (without biochar), respectively. Whereas, at Si500, the stomatal area in RHB and SMB was less than at Si250 ($p \leq 0.05$).

3.6. Electrolyte leakage and membrane stability index

The highest electrolyte leakage (0.61 %) was observed in the control, without application of Si and biochar (Fig. 4a). Among the biochar treatments, RHB resulted in the least electrolyte leakage and highest membrane stability at all Si levels. The leaf membrane stability index was enhanced by increasing Si application level from 0 to 250 mg Si kg^{-1}, reaching the highest value of 69 % in RHB300

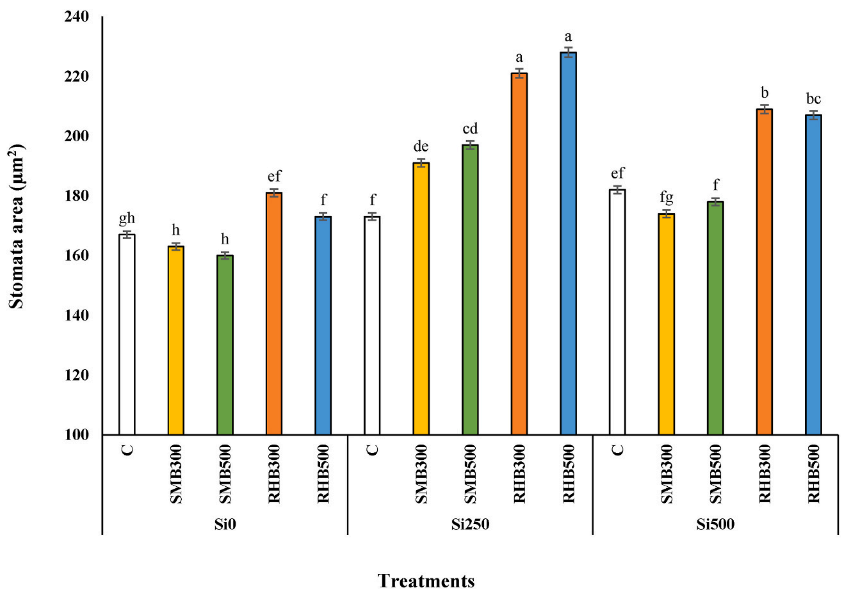

Fig. 3. Stomatal area of corn third-leaf grown in Si and biochar amended Ni-polluted soil. Leaf sections were taken from 5 to 10 mm above the leaf base. Data presented with ±SE. SMB300, sheep manure biochar prepared at 300 °C; SMB500, sheep manure biochar prepared at 500 °C; RHB300, rice husk biochar prepared at 300 °C; RHB500, rice husk biochar prepared at 500 °C. Means with the same letter do not differ significantly by LSD test at 5 % probability level.

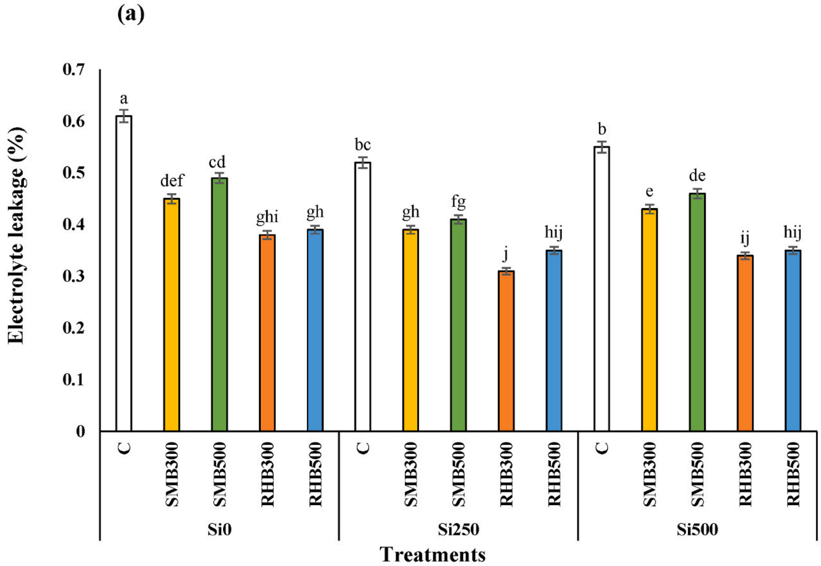

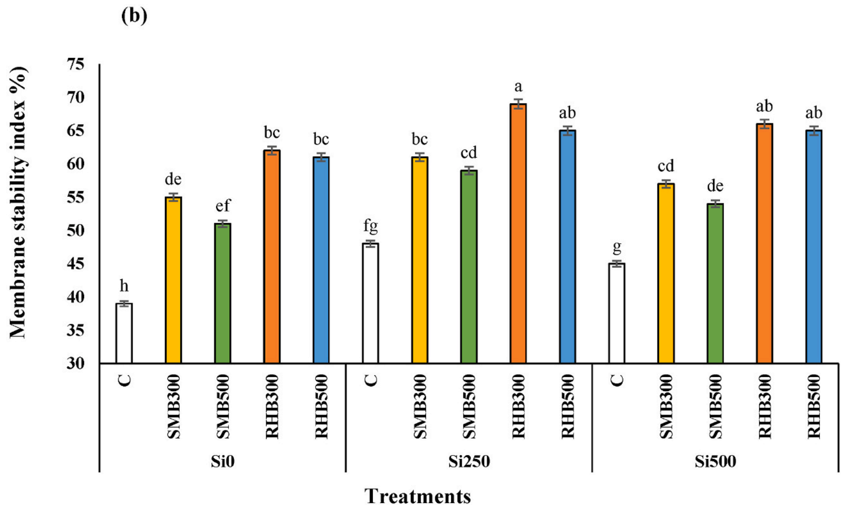

Fig. 4. Electrolyte leakage (a), and leaf membrane stability index (b) of corn third-leaf grown in Si and biochar amended Ni-polluted soil. Means with the same letter do not differ significantly by LSD test at 5 % probability level. Data presented with ±SE. SMB300, sheep manure biochar prepared at 300 °C; SMB500, sheep manure biochar prepared at 500 °C; RHB300, rice husk biochar prepared at 300 °C; RHB500, rice husk biochar prepared at 500 °C.

at Si250 treatment (Fig. 4b). Biochar temperature had no significant effect on the membrane stability index at all Si levels.

3.7. Chlorophyll and carotenoid content

The mean data of interaction effects of Si and biochar on pigments contents under Ni-polluted soil are given in Table 5. At all Si application levels, RHB (both 300 or 500 °C) had the highest chlorophyll *a* content and differed significantly from SMB and the control ($p \leq 0.05$). Also, the highest chlorophyll *a* content was observed in Si250 treatments, while Si500 was the second highest. Chlorophyll *b* content was highest at Si250 combined with biochars, with no significant difference between the different biochars. Furthermore, biochar application with no Si (Si0) had a negative effect on chlorophyll *b* content compared to Si 250. Total chlorophyll was highest in the combined Si250 and RHB biochar treatments, increasing by 145.4 and 131.8 % in RHB300 and RHB500, respectively, compared to the unamended control. At each Si application level, significant differences were observed between RHB and SMB in terms of total chlorophyll. In contrast to chlorophyll *a, b* and total, the highest carotenoid content was observed in the control followed by SMB at all of the Si levels. Furthermore, in each biochar source no significant difference ($p \leq 0.05$) was observed between 300 and 500 °C pyrolyzed temperatures.

Table 5
Interaction effect of Si and biochar application on pigment contents and enzyme activity of corn third-leaf (cv. single cross 604) grown in a Ni-polluted soil.

Si application (mg Si kg^{-1} soil)	Biochar application (3 % w/w)	Chlorophyll *a* content (mg g^{-1} FW)	Chlorophyll *b* content (mg g^{-1} FW)	Total chlorophyll content (mg g^{-1} FW)	Carotenoid content (mg g^{-1}FW)	Catalase activity (Units. mg^{-1} protein)	Peroxidase activity (Units. mg^{-1} protein)
Si0	C	0.43 ± 0.03^{h}	0.18 ± 0.01^{g}	0.61 ± 0.05^{f}	0.36 ± 0.02^{a}	1.85 ± 0.04^{a}	3.86 ± 0.07^{a}
	SMB300	1.12 ± 0.01^{f}	0.36 ± 0.01^{ef}	1.48 ± 0.02^{d}	0.21 ± 0.01^{de}	1.36 ± 0.05^{bc}	3.11 ± 0.06^{b}
	SMB500	1.22 ± 0.01^{ef}	0.40 ± 0.02^{de}	1.62 ± 0.05^{d}	0.22 ± 0.02^{cde}	1.32 ± 0.03^{c}	3.02 ± 0.03^{bc}
	RHB300	1.53 ± 0.02^{cd}	0.55 ± 0.03^{bc}	2.08 ± 0.04^{c}	0.17 ± 0.01^{efg}	1.21 ± 0.04^{de}	2.91 ± 0.04^{bcd}
	RHB500	1.44 ± 0.01^{d}	0.50 ± 0.02^{bcd}	1.94 ± 0.07^{c}	0.16 ± 0.02^{fgh}	1.19 ± 0.02^{de}	2.75 ± 0.02^{de}
Si250	C	0.71 ± 0.02^{g}	0.39 ± 0.01^{ef}	1.10 ± 0.05^{e}	0.22 ± 0.02^{cd}	1.38 ± 0.01^{b}	3.65 ± 0.05^{a}
	SMB300	1.33 ± 0.02^{e}	0.63 ± 001^{a}	1.96 ± 0.04^{c}	0.14 ± 0.02^{gh}	1.12 ± 0.03^{def}	2.89 ± 0.04^{cd}
	SMB500	1.39 ± 0.01^{de}	0.60 ± 0.02^{ab}	1.99 ± 0.03^{c}	0.16 ± 0.01^{fgh}	1.09 ± 0.01^{efg}	2.81 ± 0.02^{de}
	RHB300	1.99 ± 0.02^{a}	0.71 ± 0.02^{a}	2.70 ± 0.04^{a}	0.13 ± 0.01^{gh}	1.01 ± 0.02^{fg}	2.63 ± 0.03^{e}
	RHB500	1.86 ± 0.02^{ab}	0.69 ± 0.01^{a}	2.55 ± 0.03^{a}	0.11 ± 0.01^{h}	0.98 ± 0.04^{g}	2.60 ± 0.05^{e}
Si500	C	0.61 ± 0.01^{g}	0.28 ± 0.02^{fg}	0.89 ± 0.02^{e}	0.31 ± 0.02^{ab}	1.48 ± 0.03^{b}	3.06 ± 0.01^{bc}
	SMB300	1.26 ± 0.02^{ef}	0.35 ± 0.02^{ef}	1.61 ± 0.05^{d}	0.27 ± 0.01^{bc}	1.39 ± 0.03^{b}	2.91 ± 0.03^{bc}
	SMB500	1.24 ± 0.02^{ef}	0.36 ± 0.01^{ef}	1.60 ± 0.06^{d}	0.24 ± 0.02^{cd}	1.32 ± 0.02^{c}	2.86 ± 0.02^{cd}
	RHB300	1.71 ± 0.01^{b}	0.49 ± 0.01^{cd}	2.20 ± 0.05^{c}	0.20 ± 0.02^{def}	1.23 ± 0.04^{cd}	2.79 ± 0.01^{d}
	RHB500	1.68 ± 0.03^{bc}	0.51 ± 0.02^{bcd}	2.19 ± 0.06^{c}	0.21 ± 0.02^{de}	1.17 ± 0.02^{de}	2.76 ± 0.02^{de}

Notes: SMB300, sheep manure biochar prepared at 300 °C; SMB500, sheep manure biochar prepared at 500 °C; RHB300, rice husk biochar prepared at300 °C; RHB500, rice husk biochar prepared at 500 °C. Means in each column with the same letter do not differ significantly by LSD test at 5 % probability level. Data presented with ±SE.

3.8. Catalase and peroxidase activity

The antioxidant enzyme activity was influenced by Si and biochar application significantly ($p \leq 0.05$). The highest catalase activity (CAT) was observed in the unamended control (1.85 ± 0.04) followed by SMB at Si0 and Si500 levels (Table 5). Application of Si250 combined with biochar treatment, caused a significant decrease in CAT activity. Similarly, application of Si from 0 to 250 mg Si kg^{-1} soil declined the peroxidase activity (POX) especially in RHB (Table 5). At Si250, RHB300 and RHB500 resulted in the greatest decline in POX activity by 38.7 and 40.3 %, respectively. Overall, the lower amounts of CAT and POX activities was observed with RHB, especially at Si250 in comparison to SMB.

3.9. Relative water content

At each Si application level, the control treatment without biochar had the lowest relative water content (RWC), whereas RHB300 and RHB500 treatments were significantly higher at all Si levels (Fig. 5a). At Si250, the highest RWC was observed in RHB300, increasing by 34.8 % compared to the unamended control. In each biochar treatment, RWC in Si500 was less than Si250, especially in SMB300 and SMB500. Overall, RHB could maintain higher water content in the third-leaf of corn, in comparison to SMB at all of the Si application levels.

3.10. Plant height and total dry matter

The highest plant height (26.8 cm) was observed in the combined Si250 and RHB500 treatment, with no significant difference with RHB300 and SMB300 treatments at Si250 (Fig. 5b). Whereas the lowest plant height (14.1 cm) was obtained in the unamended Ni-polluted soil. At all Si application levels, the temperature at which RHB is prepared (300 or 500) had no significant effect ($p \leq 0.05$) on plant height of corn. Type of biochar had a noticeable effect on total dry matter production (Fig. 5c). At Si250, RHB300 had the highest total dry matter, which increased by 82.2, 120.0 and 83.1 % compared to control at Si0, Si250 and Si500, respectively. In each biochar treatment, total dry matter at Si500, had no significant difference with Si0 level. The combined Si250 and RHB300 treatment resulted in the most suitable conditions for dry matter production.

3.11. Soil Ni availability and shoot Ni concentration

The interaction effect of Si and biochar on available Ni in soil (Ni-DTPA) and Ni of corn shoot was significant ($p \leq 0.05$) (Table 6). The highest soil available Ni concentration was observed in the absence of Si and biochar application, whereas it was the lowest for the combined SMB and Si500 treatment. Likewise, the lowest Ni shoot concentration was observed in the combined SMB and Si500 treatment, with a 133 % decrease compared to the unamended control. In addition, SMB was more efficient in decreasing Ni uptake in comparison to RHB, especially when combined with Si250 or Si500.

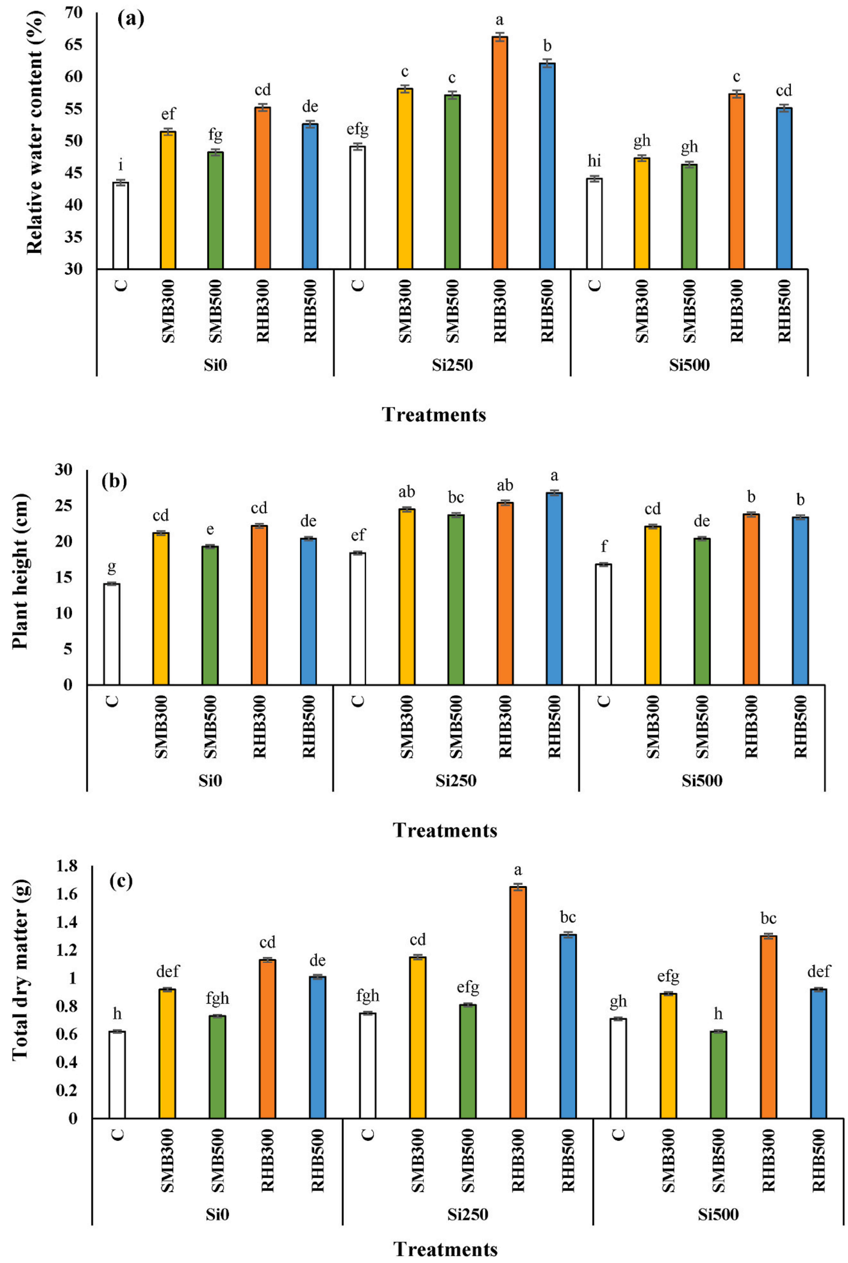

Fig. 5. Relative water content (a), plant height (b), and total dry matter (c) of corn third-leaf grown in Si and biochar amended Ni-polluted soil. Means with the same letter do not differ significantly by LSD test at 5 % probability level. Data presented with ±SE. SMB300, sheep manure biochar prepared at 300 °C; SMB500, sheep manure biochar prepared at 500 °C; RHB300, rice husk biochar prepared at 300 °C; RHB500, rice husk biochar prepared at 500 °C.

4. Discussion

4.1. Leaf dimensions and midrib area

Determination of the anatomical and biochemical changes in corn leaf is important to identify the mechanisms of Si and biochar in alleviating the negative effect of Ni as a potentially toxic element (PTE). Bijanzadeh and Kazemeini [13] showed that the area of midrib decreased between 31 and 53 % under salinity. Similar to our results, they concluded that reduction in the area of metaxylem and protoxylem of the midrib may result in lower leaf length and width in the leaf base under stress. In the current study, application of Ni as a PTE, with excessive soil concentrations caused a significant decrease in plant growth via decreasing the leaf dimensions and midrib area. In fact, the application of Si helped to alleviate the stress-related disturbance effect via maintaining the leaf area and width,

Table 6
Interaction effect of Si and biochar application on soil Ni availability (Ni-DTPA) (mg Ni kg^{-1} soil) and shoot Ni concentration (mg Ni kg^{-1} DM).

Si application (mg Si kg^{-1} soil)	Biochar application (3 % w/w)	Ni in soil (Ni-DTPA)	Ni in shoot
Si0	C	25.60 ± 0.03^{a}	10.40 ± 0.20^{a}
	SMB300	24.20 ± 0.12^{b}	7.35 ± 0.15^{bc}
	SMB500	22.00 ± 0.35^{d}	9.85 ± 0.05^{a}
	RHB300	22.30 ± 1.02^{cd}	7.55 ± 0.25^{bc}
	RHB500	20.40 ± 0.87^{f}	7.65 ± 0.75^{b}
Si250	C	22.70 ± 0.07^{c}	7.65 ± 0.05^{b}
	SMB300	21.20 ± 0.18^{e}	6.90 ± 0.60^{bc}
	SMB500	17.70 ± 0.10^{i}	6.60 ± 0.60^{cd}
	RHB300	19.20 ± 0.06^{g}	7.05 ± 0.35^{bc}
	RHB500	18.60 ± 0.06^{gh}	7.35 ± 0.35^{bc}
Si500	C	22.30 ± 0.02^{cd}	7.20 ± 0.30^{bc}
	SMB300	20.60 ± 0.19^{ef}	5.05 ± 0.65^{ef}
	SMB500	17.30 ± 0.05^{i}	4.45 ± 0.05^{f}
	RHB300	18.70 ± 0.64^{gh}	5.80 ± 0.70^{de}
	RHB500	18.40 ± 0.05^{h}	6.60 ± 0.10^{cd}

Notes: SMB300, sheep manure biochar generated at 300 °C; SMB500, sheep manure biochar generated at 500 °C; RHB300, rice husk biochar produced at 300 °C; RHB500, rice husk biochar produced at 500 °C. Means in each column with the same letter do not differ significantly by LSD test at 5 % probability level. Data presented with ±SE.

mainly when combined with RHB300. The architectural properties of the leaf such as midrib area, metaxylem and protoxylem area are related to expansion of the leaf under stress [16]. In a similar study, Adejumo et al. [41] reported that application of rice husk and sunflower waste biochar (produced at 300–350 °C) resulted in greater leaf area and weight of corn than biochars produced at 400–500 °C. In the current study, RHB at both pyrolysis temperature (300 and 500 °C) increased leaf area by 5.1–12.2 % and leaf weight by 4.7–10.5 % compared to SMB when combined with Si250 or Si500. Concomitantly, Si combined with RHB increased the leaf dimensions and midrib, metaxylem and protoxylem areas by increasing width and length of third-leaf. Overall, reduction of protoxylem and metaxylem area in midrib may be responsible for lower leaf expansion under stress due to limitation of water uptake and nutrients availability. Also, tissue architecture changes depended on severity and type of stress, type of crop and growth stage [16].

4.2. Stomatal area

Stomatal properties are one of the most important traits in photosynthetic activity and dry matter production which are affected negatively by stress [14]. In the leaf blade, the guard cells are not protected with a heavy cuticle in spite of epidermal cells which protected with a thick cuticle [15]. Consequently, the guard cells lose water directly to the atmosphere mainly under stress. Abiotic stresses usually decrease the available water in the leaves and consequently the stomatal area decreases to avoid evaporation from guard cell [42]. Zhao et al. [14] discovered that a decrease in soil moisture actually increased stomatal density; however, there was an overall reduction in stomatal aperture and size. Our results showed that, decreasing RWC of corn leaf caused by Ni toxicity, dampened stomata area drastically The reaction of stomatal area and photosynthetic properties of corn to abiotic stresses may be related to the species, RWC, nutrient availability, and the other environmental conditions [15,43]. In the current study, combination of Si250 and Si500 with RHB enhanced the stomata area due to the positive effect of these treatments in maintaining of RWC at higher levels under Ni toxicity. On the other hand, under Ni toxicity, in the combined application of Si with RHB, by increasing the length and width of the corn leaf, the surface area of the stomata increases under stress conditions compared to control.

4.3. Electrolyte leakage and membrane stability index

Electrolyte leakage shows the extent of stress damage to the plasma membrane of cells. When plants are exposed to stress, due to decreasing the turgor pressure, the plasma membrane may leak [8,44,45]. The metabolic dysfunction of plasma membranes under stress can be recognized by increasing leakage of ions, that can be determined by the efflux of electrolytes. The plant growth regulators can dampen electrolyte leakage, because of increasing RWC under stress [46]. In the current study, by increasing the RWC under Ni toxicity, electrolyte leakage increased, significantly due to application of Si with RHB. Therefore, membrane stability index as a physiological index can be used to identify the most effective Si and biochar treatments under plant stress. Bijanzadeh et al. [16], found that Si application increased membrane stability index by 12 % when plants were exposed to water stress. Our results showed using Si combined with RHB increased the leaf dimensions and midrib area which could be attributed to the limitation of cell electrolyte leakage (36.5 % decrease) and increasing membrane stability index (40.6 % increase) under Ni toxicity.

4.4. Pigments content

A reduction in the pigment's contents of leaves with Ni-toxicity has been reported by Mosa et al. [46]. Similar to our results, Boostani et al. [5], reported that soil Ni pollution led to chlorophyll *a*, chlorophyll *b*, and carotenoid depletion in spinach, and that RHB increased the chlorophyll *a and b* content more than licorice root pulp biochar. It has also been shown that PTEs, through inhibition the uptake of essential micronutrients such as Mg and Fe, can limit chlorophyll synthesis and consequently leaf area and weight [20,46]. In the present study, the chlorophyll content enhancement by application of biochar combined with Si could be attributed to the reduction of PTEs uptake and increase in nutrient uptake by the plant [5,20]. Indeed, suitable application of biochar can enhance plant dry matter production through chlorophyll content enhancement and reduction of Ni availability and uptake. The reduction of plant dry matter by Ni stress can be related to the decline in the acquisition of water and essential elements by roots, and generation of reactive oxygen species (ROS) [21].

Our results showed that in a Ni-polluted soil (300 mg Ni kg^{-1} soil) the content of chlorophyll *a*, chlorophyll *b*, and total chlorophyll in control (without Si and biochar) decreased by 245.3, 291.6 and 229.5 %, respectively. In contrast, Ni toxicity, enhanced the carotenoid content of control treatment in comparison to RHB (140.0 % increase) due to its protective effects in decreasing chlorophyll degradation [9]. The biochar pyrolysis temperature (300 or 500 °C) had no significant differences in the pigments content, while RHB at all Si levels enhanced the pigments contents compared to SMB. The much higher EC (salts content) of SMB (3.94 ± 0.06 to 4.28 ± 0.04 dS m^{-1}) in comparison to RHB may explain why it did not have such a positive effect on chlorophyll increment as compared to RHB [47].

4.4.1. Antioxidant enzyme activity

Some studies found that PTEs can enhance the activity of antioxidant CAT and POX enzymes of plant leaves to mitigate the disturbance effects of PTEs on cell membranes due to the generation of ROS [48]. In the current study, Ni toxicity increased the CAT and POX activity of control (without Si and biochar) by 34.1 and 3.86 %, respectively, compared to Si250 without biochar. Thus, it appears that Si application at 250 and 500 mg Si kg^{-1} soil resulted in more favorable plant growth conditions overcoming the toxic effects of Ni, thus decreasing the antioxidant enzyme activity. Interestingly, when Si was combined with RHB, the activity of CAT and POX decreased, but chlorophyll content improved due to the synergistic effect of Si and biochar in suppressing Ni availability. The generation of antioxidant enzymes to maintain homeostasis under stress is one of the approaches of plant tissues to mitigate the disturbance of chlorophyll production caused by ROS [10]. Increasing the enzyme activity enhances the maintenance respiration of plants to face oxygen radicals under stress, while biochar by increasing water holding in the soil creates a suitable condition for water uptake and consequently the cost of plant for enzymes activity can decrease [44]. Also, Si application has a main role in alleviating the adverse effects of stress, which includes antioxidant activity adjustment, increasing chlorophyll content and decreasing leaf transpiration, which caused the dry matter enhancement [49]. In the current study the activity of CAT and POX in different Si and biochar treatments were in the order of Si0 without biochar > Si500 without biochar > Si250 without biochar > SMB300 > SMB500 > RHB300 > RHB500. Furthermore, the enzyme activity of RHB at Si250 and Si500 was less than SMB. Also, the reduction in the enzyme activity was in line with the dry matter enhancement mainly with application of Si250 and RHB300 or RHB500.

4.4.2. RWC and plant height changes

Sattar et al. [43] found that application of Si with biochar enhanced the binary layer of silica-cuticle on corn leaf that decreases the stomatal opening under stress. RWC enhancement by biochar and Si application is also due to the regulation of the suberization and lignification of xylem vessels of leaf cells [43,50]. In stressed plants, the hydrophilic nature of Si in wall and lumen of the mesophyll cells can be associated with water retention. In the current study, the enhancement in RWC (30.6 % compared to control) due to the application of Si250 with RHB300 under Ni stress is attributed to synergistic effects of Si and biochar on plant water described above. The higher RWC in RHB in comparison to SMB may be attributed to the lower EC (salt content) of RHB at both pyrolysis temperatures. Increased presence of salts in the soil decreases the osmotic potential in plant roots, thus decreasing plant water uptake [47]. In the present study, the RWC of the corn was improved by adding biochar and, the CAT and POX activity was suppressed, concomitantly. Biochar application can increase the water holding capacity of the soil, thus generating favorable conditions for water uptake, while also decreasing the availability of Ni and consequently, the cost of antioxidant enzyme production in the plant can be declined [20,40]. Under PTE toxicity, the crop's maintenance respiration is increased because of enhanced of antioxidant enzyme production. Previous studies have reported of the positive effect of biochar on plant growth under Ni stress attributed to improvement of soil water holding capacity of soil, RWC and pH improvement [5, 6, 51]. Our results disagree to Adejumo et al. [41] who reported that application of rice husk biochar pyrolyzed at 300 °C resulted in the highest corn plant height in comparison to the same biochar produced at 400–500 °C. Whereas, our results showed that biochar pyrolysis temperature had no significant effect on plant height at Si250 and Si500 under Ni stress.

4.5. Dry matter production

Higher dry matter production under stress can be attributed to higher RWC, chlorophyll content, midrib dimensions, size of stomata, membrane stability and lower electrolyte leakage by foliar application of Si on sorghum's leaf [16]. Ibrahim et al. [12] reported that biochar application to soil contaminated with PTEs enhanced summer squash dry matter production through the organic matter and pH enhancement of the soil, which suppressed the availability of the PTEs. Biochar application to the soil can also enhance the availability of some macro and micro nutrients which positively influences dry matter production and growth rate under stress [11, 52]. Similar to our results, Sattar et al. [43] showed that Si combined with biochar improved the shoot dry weight of corn through increasing chlorophyll pigment content and RWC under water stress conditions. On the other hand, Rehman et al. [6] reported that soil Ni-pollution suppressed corn shoot dry weight, but that biochar application increased the dry matter production especially when combined with Si. In the current study, soil Ni-pollution without the application of Si and biochar, decreased the total dry matter of corn by 166.1 % in comparison to RHB300 and Si250 because of decreasing the leaf area, midrib area, total chlorophyll content, membrane stability index, and RWC by 23.4, 28.3, 68.8, 44.3 and 34.3 %, respectively.

4.5.1. Ni content

In similar study, Boostani et al. [5] reported that RHB at 2.5 % (w/w) decreased Ni availability (5–15 % reduction) and Ni concentration of spinach leaf (54–77 % reduction) in a Ni-polluted soil. In contrast to our results, they suggested that rice husk biochar pyrolyzed at 550 °C was more efficient in reduction Ni uptake and availability than biochar prepared at 350 °C. The type and growth stage of a crop, the amount and type of biochar applied to the soil, the PTEs content of the soil and the other environmental growing conditions all affect PTE uptake. Silicon also has a significant effect in suppressing plant PTE uptake due to heavy metal immobilization caused by silicate-induced pH increase in the rhizosphere [18]. Furthermore, Si application has been shown to increase PTE accumulation in the roots and limit mobilization of them to the leaves [53]. The phenomena of co-deposition of heavy metals with Si in the cell walls of roots can inhibit the heavy metals uptake and mobilization from the root cell to shoot [54]. Furthermore, by Si application, silicification mechanism in apoplast pathway creates a silica mechanical barrier, which can retard the uptake and translocation of heavy metals [55]. Wang et al. [3] declared that silicon-rich biochar had additive and positive effects on inhibiting the PTE toxicity and translocation. They suggested that the Si released from Si with biochar application can limit the gene expression of Si transport channel of roots and decrease the transport channel of Si, and consequently suppress PTE uptake, because of the same pathways for uptake of Si and heavy metals. Our results showed a synergistic effect of biochar with Si (250 and 500 mg Si kg^{-1} soil) on decreasing the concentrations of available Ni (DPTA) in the soil and Ni in the corn shoots. Reduction of available soil and shoot Ni concentrations was greater in SMB500 at Si250 and Si500 than RHB300 and RHB500, demonstrating the higher efficiency of SMB in suppressing soil Ni availability and uptake. The SMB500 had the highest ash content (60.0 ± 1.60 %) and pH (11.0 ± 0.02 %) among the biochar treatments which promotes the immobilization of Ni [5].

5. Conclusions

Results of this study demonstrated that the combined application of Si and biochar can alleviate the negative effects of soil Ni toxicity on corn dry matter production, through the changing the leaf dimensions, anatomical structure of midrib, and pigment content. Application of 250 mg Si kg^{-1} soil with RHB300 (3 % w/w), resulted in the highest dry matter production via improving the leaf area and weight, metaxylem and protoxylem areas of midrib, membrane stability index, total chlorophyll content, and relative water content. The better performance of RHB300 in dry matter production might be related to the lower soluble salt content compared to SMB, despite the fact that SMB was most effective at decreasing soil Ni availability. The leaf antioxidant enzyme activity was shown to decrease due to the synergistic positive effect of Si and biochar on physiological and biochemical properties of corn cultivated under Ni stress. Practically, we recommend that the combined application of 250 mg Si kg^{-1} soil with RHB300 was the most effective treatment in mitigating the detrimental effects of soil Ni toxicity on corn. As Ni toxicity changes the architectural characteristics of the leaf and midrib, further studies are necessary to evaluate the nutrient uptake and water flow at different Si levels and other types of biochar under Ni toxicity.

CRediT authorship contribution statement

Ehsan Bijanzadeh: Software, Investigation, Formal analysis, Conceptualization. **Hamid Reza Boostani:** Supervision, Resources, Project administration, Methodology, Data curation. **Ailsa G. Hardie:** Writing – review & editing, Writing – original draft, Supervision. **Mahdi Najafi-Ghiri:** Visualization, Validation, Project administration, Investigation.

Ethics approval and consent to participate

The study was conducted following the highest ethical standards. The data presented in this manuscript are accurate and authentic.

Data availability statement

All the data of the article are available in the text.

Funding

The authors received no financial support for the research, authorship, or publication of this article.

Declaration of competing interest

The authors declare that they have no known competing financial interests or personal relationships that could have appeared to influence the work reported in this paper.

Acknowledgements

The authors thank the College of Agriculture and Natural Resources of Darab, Shiraz University, Iran for providing the facilities and

support.

References

[1] E. Houshyar, X. Wu, G. Chen, Sustainability of wheat and maize production in the warm climate of southwestern Iran: an emergy analysis, J. Clean. Prod. 172 (2018) 2246–2255.
[2] FAO. Food, Supply Database, 2022. wwwfaoorg.
[3] Y. Wang, K. Zhang, L. Lu, X. Xiao, B. Chen, Novel insights into effects of silicon-rich biochar (Sichar) amendment on cadmium uptake, translocation and accumulation in rice plants, Environ. Pollut. 265 (2020) 114772.
[4] B. Wang, C. Chu, H. Wei, L. Zhang, Z. Ahmad, S. Wu, Ameliorative effects of silicon fertilizer on soil bacterial community and pakchoi (*Brassica chinensis* L.) grown on soil contaminated with multiple heavy metals, Environ. Pollut. 267 (2020) 115411.
[5] H.R. Boostani, M. Najafi-Ghiri, A. Mirsoleimani, The effect of biochars application on reducing the toxic effects of nickel and growth indices of spinach (*Spinacia oleracea* L.) in a calcareous soil, Environ. Sci. Pollut. Res. 26 (2019) 1751–1760.
[6] M.Z. Rehman, M. Rizwan, S. Ali, N. Fatima, B. Yousaf, A. Naeem, Contrasting effects of biochar, compost and farm manure on alleviation of nickel toxicity in maize (*Zea mays* L.) in relation to plant growth, photosynthesis and metal uptake, Eco. Envi. Safety 133 (2016) 218–225.
[7] Y. Wang, B. Zhong, M. Shafi, J. Ma, J. Guo, J. Wu, Effects of biochar on growth, and heavy metals accumulation of moso bamboo (*Phyllostachy pubescens*), soil physical properties, and heavy metals solubility in soil, Chemo 219 (2019) 510–516.
[8] W. Begum, S. Rai, S. Banerjee, S. Bhattacharjee, M.H. Mondal, A. Bhattarai, A comprehensive review on the sources, essentiality and toxicological profile of nickel, RSC Adv. 12 (2022) 9139–9153.
[9] M. Gholizadeh, X. Hu, Removal of heavy metals from soil with biochar composite: a critical review of the mechanism, J. Environ. Chem. Eng. 9 (2021) 105830.
[10] H.S. Kim, K.R. Kim, H.J. Kim, J.H. Yoon, J.E. Yang, Y.S. Ok, Effect of biochar on heavy metal immobilization and uptake by lettuce (*Lactuca sativa* L.) in agricultural soil, Envi, Earth Sci. 74 (2015) 1249–1259.
[11] A. Pescatore, C. Grassi, A.M. Rizzo, S. Orlandini, M. Napoli, Effects of biochar on berseem clover (*Trifolium alexandrinum* L.) growth and heavy metal (Cd, Cr, Cu, Ni, Pb, and Zn) accumulation, Chemo. 287 (2022) 131986.
[12] E.A. Ibrahim, M.A. El-Sherbini, E.M.M. Selim, Effects of biochar on soil properties, heavy metal availability and uptake, and growth of summer squash grown in metal-contaminated soil, Sci. Hort. 301 (2022) 111097.
[13] E. Bijanzadeh, S.A. Kazemeini, Tissue architecture changes of expanding barley (*Hordeum vulgare* L.) leaf under salt stress, Aust. J. Crop. Sci. 8 (2014) 1373–1379.
[14] W. Zhao, Y. Sun, R. Kjelgren, X. Liu, Response of stomatal density and bound gas exchange in leaves of maize to soil water deficit, Acta Physiol. Plant. 37 (2015) 1–9.
[15] S. Wu, B. Zhao, Using clear nail polish to make Arabidopsis epidermal impressions for measuring the change of stomatal aperture size in immune response, Methods Mol. Biol. 1578 (2017) 243–248.
[16] E. Bijanzadeh, V. Barati, T.P. Egan, Foliar application of sodium silicate mitigates drought stressed leaf structure in corn (*Zea mays* L.), South Afr. J. Botany. 147 (2022) 8–17.
[17] M.J. Hodson, D.E. Evans, Aluminium–silicon interactions in higher plants: an update, J. Exp. Bot. 71 (2020) 6719–6729.
[18] C. Ma, K. Ci, J. Zhu, Z. Sun, Z. Liu, X. Li, Impacts of exogenous mineral silicon on cadmium migration and transformation in the soil-rice system and on soil health, Sci. Total Environ. 759 (2021) 143501.
[19] D.K. Tripathi, P. Rai, G. Guerriero, S. Sharma, F.J. Corpas, V.P. Singh, Silicon induces adventitious root formation in rice under arsenate stress with involvement of nitric oxide and indole-3-acetic acid, J. Exp. Bot. 72 (2021) 4457–4471.
[20] H.R. Boostani, A.G. Hardie, M. Najafi-Ghiri, Chemical fractions and bioavailability of nickel in a Ni-treated calcareous soil amended with plant residue biochars, Arch. Agro. Soil Sci. 66 (2019) 730–742.
[21] P.M.A. Ramzani, S. Anjum, F. Abbas, M. Iqbal, A. Yasar, M.Z. Ihsan, Potential of miscanthus biochar to improve sandy soil health, in situ nickel immobilization in soil and nutritional quality of spinach, Chemo 185 (2017) 1144–1156.
[22] H.R. Boostani, A.G. Hardie, M. Najafi-Ghiri, E. Bijanzadeh, Investigation of interaction effects of biochars and silicon on growth and chemical composition of *Zea mays* L. in a Ni-polluted calcareous soil, Sci. Rep. 13 (2023) 19935.
[23] M.I. Al-Wabel, A.R. Usman, A.H. El-Naggar, A.A. Aly, H.M. Ibrahim, S. Elmaghraby, Conocarpus biochar as a soil amendment for reducing heavy metal availability and uptake by maize plants, Saudi J. Biol. Sci. 22 (2015) 503–511.
[24] A.I. Amouei, Z. Yousefi, A.H. Mahvi, K. Naddafi, M. Tahmasbizadeh, Heavy metal concentrations in industrial, agricultural, and highway soils in northern Iran, Environ. Justice 5 (2012) 153–157.
[25] IUSS Working Group, World Reference Base for Soil Resources. International Soil Classification System for Naming Soils and Creating Legends for Soil Maps", 2014.
[26] Y. Sun, B. Gao, Y. Yao, J. Fang, M. Zhang, Y. Zhou, H. Chen, L. Yang, Effects of feedstock type, production method, and pyrolysis temperature on biochar and hydrochar properties, Chem. Engin. J. 240 (2014) 574–578.
[27] X. Yang, J. Liu, K. Mc Grouther, H. Huang, K. Lu, X. Guo, L. He, X. Lin, L. Che, Z. Ye, Effect of biochar on the extractability of heavy metals (cd, cu, pb, and zn) and enzyme activity in soil, Environ. Sci. Pollut. Res. 23 (2016) 974–984.
[28] A.A. Abdelhafez, J. Li, M.H. Abbas, Feasibility of biochar manufactured from organic wastes on the stabilization of heavy metals in a metal smelter contaminated soil, Chemo 117 (2014) 66–71.
[29] J.C. Zadoks, T.T. Chang, C.F. Konzak, A decimal code for the growth stages of cereals, Weed Res. 14 (1974) 415–421.
[30] Y. Hu, H. Schnyder, U. Schmidhalter, Carbohydrate deposition and partitioning in elongating leaves of wheat under saline soil conditions, Func. Plant Biol. 27 (2000) 363–370.
[31] Y. Hu, J. Fromm, U. Schmidhalter, Effect of salinity on tissue architecture in expanding wheat leaves, Planta 220 (2005) 838–848.
[32] C. Hachez, M. Moshelion, E. Zelazny, D. Cavez, F. Chaumont, Localization and quantification of plasma membrane aquaporin expression in maize primary root: a clue to understanding their role as cellular plumbers, Plant Mol. Biol. 62 (2006) 305.
[33] D. Arnon, Copper enzymes in isolated polyphenol oxidase in Beta vulgaris, Plant Phy 24 (1949) 1–16.
[34] H.K. Lichtenthaler, Chlorophylls and carotenoids: pigments of photosynthetic biomembranes, Methods Enzm 148 (1987) 350–382.
[35] H. Aebi, [13] Catalase in vitro, Methods Enzy 105 (1984) 121–126.
[36] B. Chance, A. Maehly, [136] Assay of Catalases and Peroxidases, 1955.
[37] H. Gong, K. Chen, The regulatory role of silicon on water relations, photosynthetic gas exchange, and carboxylation activities of wheat leaves in field drought conditions, Acta Phy. Plant. 34 (2012) 1589–1594.
[38] S. Rao, A. Qayyum, A. Razzaq, M. Ahmad, I. Mahmood, A. Sher, Role of foliar application of salicylic acid and l-tryptophan in drought tolerance of maize, J. Animal Plant Sci. 22 (2012) 768–772.
[39] S. Machado, G.M. Paulsen, Combined effects of drought and high temperature on water relations of wheat and sorghum, Plant Soil 233 (2001) 179–187.
[40] H. Chapman, Leaf and SOIL Analysis in Citrus Orchards. California Agricultural Experiment Station. Extension Service manual 25, Univ. of California Press, Berkeley, CA, 1960.
[41] S. Adejumo, M. Owolabi, I. Odesola, Agro-physiologic effects of compost and biochar produced at different temperatures on growth, photosynthetic pigment and micronutrients uptake of maize crop, African J. Agr. Res. 11 (2016) 661–673.
[42] H. Bi, N. Kovalchuk, P. Langridge, P.J. Tricker, S. Lopato, N. Borisjuk, The impact of drought on wheat leaf cuticle properties, BMC Plant Biol. 17 (2017) 1–13.

[43] A. Sattar, A. Sher, M. Ijaz, S. Ul-Allah, M. Butt, M. Irfan, Interactive effect of biochar and silicon on improving morpho-physiological and biochemical attributes of maize by reducing drought hazards, J. Soil Sci. Plant Nutr. 20 (2020) 1819–1826.
[44] W.M. Semida, H.R. Beheiry, M. Sétamou, C.R. Simpson, T.A. Abd El-Mageed, M.M. Rady, Biochar implications for sustainable agriculture and environment: a review, South Afr. J. Bot. 127 (2019) 333–347.
[45] M. Sedaghat, Z. Tahmasebi-Sarvestani, Y. Emam, A. Mokhtassi-Bidgoli, Physiological and antioxidant responses of winter wheat cultivars to strigolactone and salicylic acid in drought, Plant Phy. Bio. 119 (2017) 59–69.
[46] A. Mosa, M.F. El-Banna, B. Gao, Biochar filters reduced the toxic effects of nickel on tomato (*Lycopersicon esculentum* L.) grown in nutrient film technique hydroponic system, Chemo 149 (2016) 254–262.
[47] M. Qadir, S. Schubert, Degradation processes and nutrient constraints in sodic soils, Land Degr. Dev. 13 (2002) 275–294.
[48] H.R. Boostani, M. Najafi-Ghiri, M. Safizadeh, Can addition of biochar and zeolite to a contaminated calcareous soil mitigate the Pb-toxicity effects on Spinach (*Spinacia oleracea* L.) growth? Commun. Soil Sci. Plant Anal. 52 (2021) 136–148.
[49] M.F. Seleiman, Y. Refay, N. Al-Suhaibani, I. Al-Ashkar, S. El-Hendawy, E.M. Hafez, Integrative effects of rice-straw biochar and silicon on oil and seed quality, yield and physiological traits of *Helianthus annuus* L. grown under water deficit stress, Agronomy 9 (2019) 637.
[50] R.A. Flores, E.M. Arruda, J.P. Souza Junior, R. de Mello Prado, A.C.A. Santos, A.S. Aragão, Nutrition and production of *Helianthus annuus* in a function of application of leaf silicon, J. Plant Nutr. 42 (2019) 137–144.
[51] F. de Tombeur, J. Cooke, L. Collard, D. Cisse, F. Saba, D. Lefebvre, Biochar affects silicification patterns and physical traits of rice leaves cultivated in a desilicated soil (*Ferric Lixisol*), Plant Soil 460 (2021) 375–390.
[52] M. Najafi-Ghiri, E. Bijanzadeh, F. Bahadori, Effect of wheat-derived biochar on soil nutrients availability and nutrients uptake by two Safflower (*Carthamus tinctorius* L.) cultivars under water stress, Commun. Soil Sci. Plant Anal. 53 (2022) 1592–1606.
[53] T. Babu, P. Nagabovanalli, Effect of silicon amendment on soil-cadmium availability and uptake in rice grown in different moisture regimes, J. Plant Nutr. 40 (2017) 2440, 1457.
[54] S. Wang, F. Wang, S. Gao, Foliar application with nano-silicon alleviates Cd toxicity in rice seedlings, Environ. Sci. Pollut. Res. 22 (2015) 2837–2845.
[55] H. Etesami, B.R. Jeong, Silicon (Si): review and future prospects on the action mechanisms in alleviating biotic and abiotic stresses in plants, Eco. Envi. Safety 147 (2018) 881–896.